Dawn-dusk asymmetries, ion spectra, and sources in the northward interplanetary magnetic field plasma sheet

S. Wing
Applied Physics Laboratory, Johns Hopkins University, Laurel, Maryland, USA

J. R. Johnson
Princeton Plasma Physics Laboratory, Princeton University, Princeton, New Jersey, USA

P. T. Newell and C.-I. Meng
Applied Physics Laboratory, Johns Hopkins University, Laurel, Maryland, USA

Received 17 February 2005; revised 18 April 2005; accepted 18 May 2005; published 20 August 2005.

[1] During periods of northward IMF, plasma sheet ions often have two components: hot (magnetospheric origin) and cold (magnetosheath origin). The temperatures of the cold-component ions are ~30–40% higher in the dawn sector compared to the dusk sector, implying the dawnside magnetosheath ion heating of ~30–40%. As a result, the magnetosheath ions are less distinguishable from the hot-component ions, which have lower temperatures on the dawnside, leading to a higher occurrence of the ions having (apparent) one-component distribution. As the duration of the hourly averaged IMF being northward (Δt) increases from 1 to 10 hours, the occurrence of two-component ions increases from 65% to 83% in the dusk flank, but in the dawn flank it remains relatively stable at around 45%. In contrast, the occurrence of ions best characterized by kappa (κ) distribution increases from 25% to 35% in the dawn flank whereas in the dusk flank it remains relatively insensitive to Δt (10%). The occurrence of a one-component Maxwellian distribution appears to be most pronounced in the region of the plasma sheet close to the midnight meridian, and these ions appear to be characteristic of the nominal plasma sheet (hot component) ions. The densification of the plasma sheet, as Δt increases, mainly results from the influx of the magnetosheath ions. However, the cooling of the plasma sheet ions can be attributed not only to the influx of the cold magnetosheath ions but also to the cooling of the nominal plasma sheet ions. The dawn-dusk asymmetries observed in the cold magnetosheath ion profiles should provide constraints that can help determine the roles of various proposed magnetosheath ion entry mechanisms.

Citation: Wing, S., J. R. Johnson, P. T. Newell, and C.-I. Meng (2005), Dawn-dusk asymmetries, ion spectra, and sources in the northward interplanetary magnetic field plasma sheet, *J. Geophys. Res.*, *110*, A08205, doi:10.1029/2005JA011086.

1. Introduction

[2] Satellite observations in the magnetotail show that plasma sheet ions are colder and denser during periods of northward IMF compared with southward IMF [e.g., *Terasawa et al.*, 1997; *Fujimoto et al.*, 1998; *Stenuit et al.*, 2002; *Øieroset et al.*, 2005]. This trend has also been observed in the inferred 2-D plasma sheet ion profiles obtained from DMSP satellites in the ionosphere [*Wing and Newell*, 2002].

[3] In situ observations reveal that there is a dawn-dusk asymmetry in the cold, dense ion population. Along the dusk flank, just inside the magnetosphere, the ion spectra often exhibit two components. One component has a lower temperature, which is similar to that of the magnetosheath, and the other has a higher temperature, which is believed to be similar to that of the nominal plasma sheet. In contrast, along the dawn flank, ion spectra often exhibit just one component with a broad peak. Examples of the ion energy-time spectrograms that show this asymmetry along the dawn and dusk flanks are given by *Fujimoto et al.* [1998].

[4] *Hasegawa et al.* [2003] examined the Geotail ion and electron distributions at low latitude inside the magnetosphere near the magnetopause boundary at dawn and dusk and much of the dayside. They observed the same dawn-dusk asymmetry during periods of northward IMF. Figure 1 displays the typical ion distributions obtained near the dawn and dusk flanks [from *Hasegawa et al.*, 2003]. Figure 1a shows the ion distribution observed when Geotail was near the dusk sector. It shows that the ion low-energy/low-temperature component is fairly isotropic and similar to that of the magnetosheath

Copyright 2005 by the American Geophysical Union.
0148-0227/05/2005JA011086$09.00

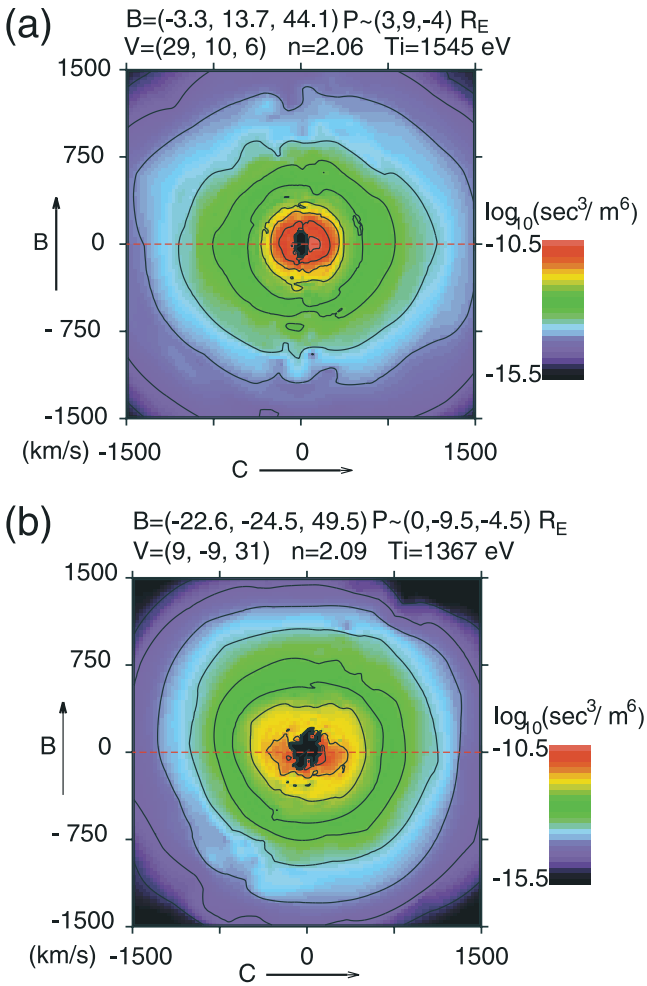

Figure 1. Ion distribution functions in the mixed region where cold magnetosheath-like and hot magnetospheric ions are simultaneously observed in (a) the dusk flank and (b) the dawn flank. Shown are the slices of the flow in the BC planes, where the Y axis = B = aligned with the magnetic field and the X axis = C = perpendicular to the magnetic field. The cold and hot components in the dusk flank (Figure 1a) are fairly isotropic. However, in the dawn flank (Figure 1b) the hot component is fairly isotropic, but the cold component shows evidence of heating in the direction perpendicular to the magnetic field. B is magnetic field (nT), P is satellite coordinate (R_E), V is ion velocity (km/s), n is ion density (cm^{-3}), and Ti is ion temperature (eV) [from *Hasegawa et al.*, 2003].

distribution [e.g., *Fujimoto et al.*, 1998]. The high-energy/high-temperature component is also isotropic and similar to that of the ions in the nominal plasma sheet. This distribution is consistent with Wind satellite observations at the low-latitude dusk flank [*Phan et al.*, 1997]. An example of a typical ion distribution observed near the dawn sector is shown in Figure 1b. In contrast to the dusk distribution, the low-energy/low-temperature component is anisotropic with $T_\perp > T_\parallel$, while the high-energy component remains isotropic as on the dusk flank. That only the cold component is heated suggests that the magnetosheath ions have been heated in the direction perpendicular to the magnetic field direction. In the follow-up study, *Hasegawa et al.* [2004a] investigated the frequency of observing one- or two-component ion distribution as a function of local time. The result is plotted in Figure 2 [from *Hasegawa et al.*, 2004a]. In Figure 2, if the ion energy flux has two peaks with one peak below and one above 3 keV, the two peaks are plotted on the same ordinate with a green and a red dot, respectively. Otherwise, the spectrum is classified as having one component, and a black dot indicates its peak energy. Figure 2 shows that there are significantly more two-component ions (red and green dots) in the dusk flank compared with in the dawn flank. Conversely, there are more one-component ions (black dots) in the dawn than in the dusk flank. On the dawnside, when two-component ion distributions are observed, the separation between the hot and cold components (red and green dots) is narrower in the energy/temperature space. Indeed, when observed, the typical cold component appears to have higher temperature on the dawn flank than on the dusk flank, while the hot component appears to have lower temperature in the dawn flank than in the dusk flank.

[5] The dawn-dusk asymmetric heating of the magnetosheath ions observed near the magnetopause should leave signatures on the plasma sheet ion population because once inside the magnetosphere, the magnetosheath ions will gradient and curvature drift duskward and $\mathbf{E} \times \mathbf{B}$ drift earthward. It would be expected that even if only the perpendicular component gets heated during the magnetopause entry, after several bounces and crossings of the current sheet, the higher temperature may spread to other pitch angles through pitch angle scattering in the current sheet [*Lyons and Speiser*, 1982]. Thus, away from the magnetopause, the evidence of heating may be found in all pitch angles.

[6] We have developed a method for inferring plasma sheet ion temperature, density, and pressure from the ionospheric observations [*Wing and Newell*, 1998]. In the present study, we used this method and DMSP observations to further investigate the nature of this dawn-dusk asymmetry. The advantage of this method is that, with the abundance of the DMSP data, the plasma sheet can be "imaged" fairly quickly, and good statistics can be obtained in a relatively short time. Moreover, the evolution of these plasma sheet parameters can be investigated as a function of the duration of northward IMF. The following section discusses the data set used in this study. Section 3 briefly reviews the method for inferring plasma sheet properties from the ionospheric observations. Section 4 presents the statistical profiles of the inferred plasma sheet ion density and temperature for northward IMF. Section 5 presents the evolution of those two parameters. Finally, section 6 discusses and summarizes our findings, which provide significant observational constraints for the various proposed entry mechanisms of the magnetosheath ions into the magnetotail.

2. Data Set

[7] This study used data from the SSJ4 instrument on board Defense Meteorological Satellite Program (DMSP)

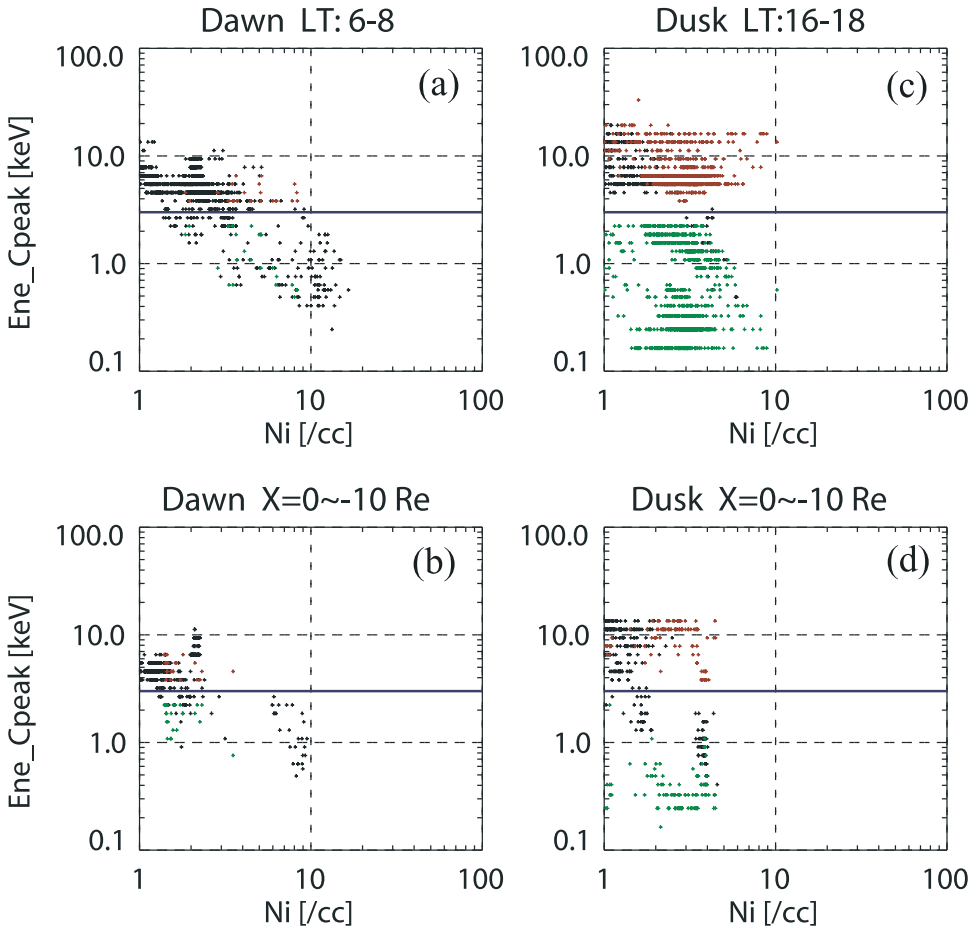

Figure 2. Ion energy spectrum behavior in the mixed region during extended northward IMF periods in the (a and b) dawn and (c and d) dusk flanks. For each data sample, if the ion energy spectrum has a count rate (energy flux) peak both below and above 3 keV, the higher and lower peak energies are plotted as red and green dots, respectively. Otherwise, the energy at which the count rate reaches maximum is plotted as a black dot. There is a clear dawn-dusk asymmetry. There are more two-component ions on the duskside than on the dawnside. Conversely, there are more one-component ions on the dawnside than on the duskside. On the dawnside, the hot and cold components (red and green dots) are closer together in energy/temperature space [from *Hasegawa et al.*, 2004a].

satellites F8, F9, F10, and F11 for the entire year of 1992. In 1992, there were at least three DMSP satellites in operation simultaneously (F8, F10, and either F9 or F11) and for one month, March, all four were in operation. As 1992 is near solar maximum, this choice of data set introduces some biases to those plasma sheet parameters that have solar cycle dependences. For example, the average solar wind density is well correlated with the average plasma sheet density; hence both values should be higher near solar maximum [*Borovsky et al.*, 1998; *Papitashvili et al.*, 2000].

[8] The SSJ4 instrumental package included on all recent DMSP flights uses curved figure electrostatic analyzers to measure ions and electrons from 32 eV to 30 keV in logarithmically spaced steps [*Hardy et al.*, 1984]. Because of its upward pointing and limited pitch angle resolution, DMSP SSJ4 measures only highly field-aligned precipitating particles at an altitude of roughly 835 km. NASA NSSDC OMNIWeb provides the IMP 8 hourly average solar wind data.

3. Method for Inferring Plasma Sheet Ion Temperature, Density, and Pressure From Ionospheric Observations

[9] The method for inferring the plasma sheet temperature, density, and pressure from the DMSP SSJ4 measurements has been described fully elsewhere [*Wing and Newell*, 1998, 2000] and is briefly summarized here.

[10] It has been known for more than two decades that energetic ions observed in the topside ionosphere are isotropic above a certain latitude [e.g., *Bernstein et al.*, 1974]. Likewise, an overwhelming number of in situ observations in the plasma sheet tailward of $\sim$8–10 R_E that indicate that plasma is nearly isotropic irrespective of activity levels [e.g., *Kistler et al.*, 1992; *Spence et al.*,

1989; *Huang and Frank*, 1994; *Sarris et al.*, 1981]. As a result, density, temperature, and pressure are conserved along the magnetic field line. The ions maintain their isotropy by pitch angle scattering in the tail current sheet [*Lyons and Speiser*, 1982]. The physical mechanism is quite simple: ions cannot maintain their magnetic moments while traversing field lines that have a radius of curvature that is a significant fraction of their gyroradii [*Sergeev et al.*, 1993]. In the region where the curvature of the field line is small, the cross-tail current bends magnetic field lines enough to cause pitch angle scattering whenever an ion crosses the current sheet [*Lyons and Speiser*, 1982; *Sergeev et al.*, 1993]. Nearer to Earth (typically earthward of $\sim$8–10 R_E, although it varies with magnetic activity), the field line becomes more dipolar and the pitch angle scattering ceases. As a result, the plasma becomes trapped, the particle precipitation drops drastically, and our method does not work in this region. This is the basis for the identification of the latitude of the equatorward isotropy boundary in the ionosphere (b2i) or equivalently the earthward boundary of the central plasma sheet (CPS) [*Newell et al.*, 1996, 1998; *Sergeev et al.*, 1993]. Because b2i (expressed in the magnetic latitude in degrees) has a local time variation, it is normalized to its midnight value.

[11] The earthward boundary of the plasma sheet moves closer to the Earth, and the magnetotail magnetic field line becomes more stretched with the increasing magnetic activity. Hence b2i decreases with increasing magnetic activity (see, for example, the plot of *Kp* versus b2i given by *Wing and Newell* [2003, Figure 1]). An important consequence of this result is that b2i can be used to indicate the stretching of the field lines and to improve the magnetic field model. In fact, *Sergeev et al.* [1993] confirm this relationship by showing that there is a 0.9 correlation coefficient between the latitude of the ion isotropy boundary (or b2i) and the tail inclination angle measured in the same local time sector by GOES geosynchronous satellites. Therefore b2i can be used to modify and improve the ionosphere–magnetosphere tail mapping of the T89 magnetic field model [*Tsyganenko*, 1989]. The unmodified T89 model uses *Kp*, a 3-hour averaged index, as one of the input parameters, but the modified T89 model uses an additional input parameter, b2i, which is an instantaneous index. In the modified T89 model, the b2i is used as an index to modify the tail current slightly so that the tail field line stretching empirically agrees well with that of GOES observations [see *Sergeev and Gvozdevsky*, 1995, Figure 7]. The mapping accuracy from the ionosphere to the equatorial plane in the original T89 model has been investigated by *Pulkkinen and Tsyganenko* [1996]. They find that the mapping errors are generally small, <1 R_E in the equatorial plane for $Kp < 3$ for magnetic latitude (mlat) <69° (in SM coordinate system). For mlat >69° (for the region further down the tail and closer to open field lines), they find that the error is <1 R_E in the x direction and <3 R_E in the y direction. With b2i, the modified T89 model provides an even more accurate and instantaneous field line tail mapping.

[12] In addition to good ionosphere-magnetosphere mapping, our method of inferring plasma sheet ion properties calls for other steps that have to be performed carefully. Electron acceleration events accelerate electrons downward and retard ions. These events have to be excluded from the data because they distort the plasma sheet particle spectra, resulting in distributions that do not represent those in the plasma sheet. An algorithm developed by *Newell et al.* [1996] to identify the electron acceleration events is used. Then, each individual ion spectrum that is not an electron acceleration event is fitted to three spectral forms: (1) one-component Maxwellian, (2) two-component Maxwellian, and (3) kappa (κ) distribution [e.g., *Vasyliunas*, 1971; *Christon et al.*, 1988, 1989]. In the spectra of ions with energy <30 keV, a κ distribution with $\kappa > 10$ is hardly distinguishable from a Maxwellian distribution. Because of the limited number of good points after noise removal, the two-component κ fit, which requires more free parameters, may be less reliable and hence was not attempted in this study [*Wing and Newell*, 1998]. Figure 3 shows an example of spectra that fit each type of the distribution function. From these three fits, the best fit is selected according to reduced χ^2 and $F\chi$ tests, which takes into account the number of free parameters used [*Bevington*, 1969]. The spectrum is discarded if no fit is statistically valid. Unlike moment calculations, which are widely used, fitting the differential energy flux, $dj(E)/dE$, to a phase space density function takes into account ions outside the detector's energy range. The plasma sheet ions have been observed to have an energy range from a few eV up to a few hundred keV or higher [e.g., *Kistler et al.*, 1992; *Christon et al.*, 1988, 1989; *Lennartsson and Shelley*, 1986; *Meng et al.*, 1981]. As expected, the density obtained using our method is higher than that obtained from the moment calculation.

[13] In the 2-D equatorial profiles, the average density, temperature, and pressure are calculated in 1 $R_E \times 1$ R_E bins. Valid values are given only if there are at least 10 good points present in each bin. For example, to obtain the average parameter of the one-component Maxwellian ion population, each bin must have at least 10 good points (spectra) of one-component Maxwellian fits. In addition, each spectrum is considered good only if there is another good spectrum (as determined by the fit criteria mentioned above) with similar distribution found within 4 sec (30 km in ionosphere). These criteria are relaxed when calculating the statistic for the occurrence of the type of distribution, i.e., one-component Maxwellian, two-component Maxwellian, and κ distributions. For this, valid values are given only if there are at least three good points present in each bin. Because of the differences in the criteria, the 2-D profiles showing the probability of occurrence of ion distribution types appear to have more spatial coverage than the 2-D profiles showing the average density, temperature, and pressure (in sections 4 and 5).

[14] In the present paper, the temperature reported for the κ distribution is the generalized temperature, which is given as follows. The κ distribution is given by

$$f_k(W) = n\left(\frac{m}{2\pi\kappa W_0}\right)^{\frac{3}{2}}\frac{\Gamma(\kappa+1)}{\Gamma\left(\kappa-\frac{1}{2}\right)}\left(1+\frac{W^*}{\kappa W_0}\right)^{-(\kappa+1)} \quad (1)$$

where n = density, m = mass, $W^* = (\sqrt{W} - \sqrt{W_s})^2$, W = energy = 0.5 mv^2, v = velocity, and W_s = shift energy [*Baumjohann and Treumann*, 1997]. W_0 is the particle

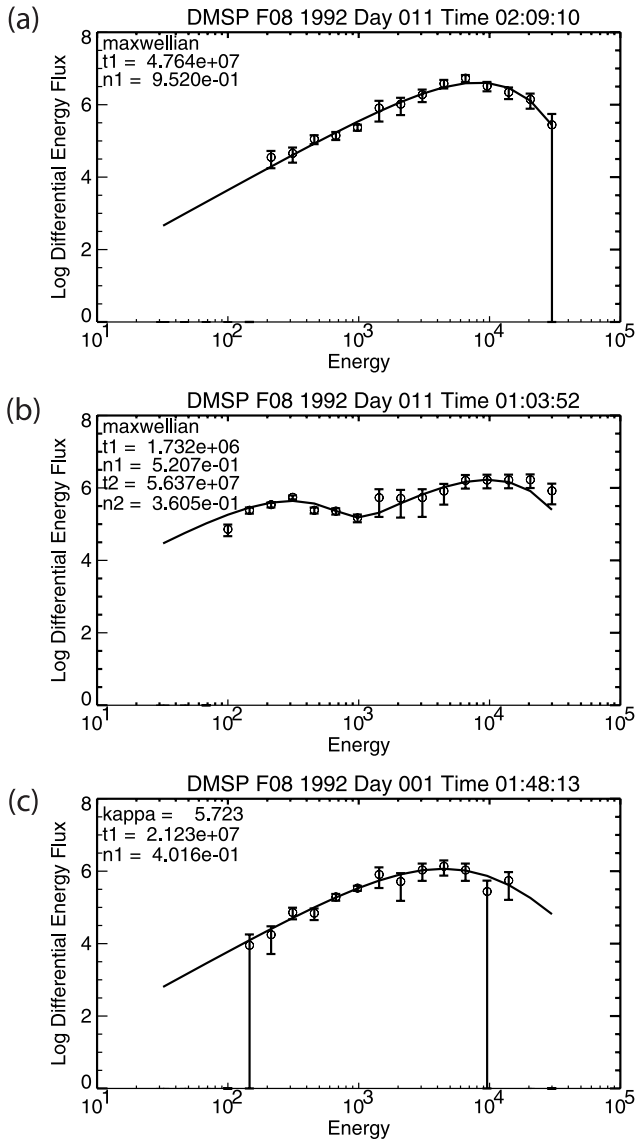

Figure 3. An example of the differential energy flux with (a) one-component Maxwellian, (b) two-component Maxwellian, and (c) κ distributions.

energy peak of the distribution and can be related to the average thermal energy by

$$W_0 = k_B T\left(1 - \frac{3}{2\kappa}\right) \tag{2}$$

Note that for $\kappa \gg 1$, equation (2) reverts back to the simple Maxwellian case. Thus the generalized temperature is

$$k_B T = \frac{2\kappa W_0}{2\kappa - 3} \tag{3}$$

The method does have limitations. One of the more significant ones is that because of the uncertainty in the ionosphere-magnetosphere mapping, the method is not suitable for studying microscale features of the plasma sheet, but it should be adequate for macroscale or global phenomena. However, previous studies have shown that the plasma sheet cooling and densification during periods of northward IMF are macroscale phenomena [*Stenuit et al.*, 2002; *Øieroset et al.*, 2005].

[15] Extensive comparisons of the inferred plasma sheet density, temperature, and pressure with those obtained from in situ measurements [e.g., *Lennartsson and Shelley*, 1986; *Lennartsson*, 1992; *Baumjohann et al.*, 1989, 1990; *Huang and Frank*, 1994; *Angelopoulos et al.*, 1993; *Angelopoulos*, 1996; *Spence et al.*, 1989] show fairly good agreement [*Wing and Newell*, 1998] with some caveats as discussed above and in *Wing and Newell* [1998, 2003].

4. Characteristics of the Northward IMF Plasma Sheet Cold and Hot Components

[16] We applied the method described in section 3 to the DMSP data for the entire year of 1992. In this section, the statistical northward IMF plasma sheet profile was constructed by selecting the DMSP observations obtained when the simultaneous hourly averaged IMF is northward. (Section 5 examines the evolution of the plasma sheet as IMF turns northward and remains northward for 1 to 10 hours). Figure 4 shows the resulting northward IMF 2-D ion density and temperature profiles on the equatorial plane. In this study, all the observations are mapped to the equatorial plane and hence herein the plasma sheet refers to the central plasma sheet (CPS). Figure 4 affirms that the plasma sheet gets cold and dense during periods of northward IMF (for example, Figure 4 can be compared with the southward IMF ion density and profiles given by *Wing and Newell* [2002]). As previously shown, in the inner plasma sheet region, around 8–10 R_E, the plasma sheet is hotter in the dusk-midnight sector than in the midnight-dawn sector [*Wing and Newell*, 1998, 2002]. This difference can be attributed to the gradient and curvature drift, which moves hotter ions duskward, as clearly demonstrated in some model calculations [*Spence and Kivelson*, 1993; *Wang et al.*, 2001, 2002, 2003].

[17] In addition to the dawn-dusk asymmetry in the inner edge of the plasma sheet, which results from the ion motion, there are other dawn-dusk asymmetries further down the tail in the flanks. As a start, Figure 4 shows that the density is higher along the dawn flank than along the dusk flank. The density peaks and temperature minima along the flanks have been previously identified as signatures of magnetosheath ion entry [e.g., *Wing and Newell*, 1998, 2002]. These signatures have been produced in the *Wang et al.* [2001, 2002, 2003] model and the Finite Width Magnetotail Convection (FWMC) model [*Spence and Kivelson*, 1993]. These models have two ion sources: (1) magnetosheath ions (cold), along the flank magnetopause, and (2) nominal plasma sheet ions (hot), which originate further down the tail (tailward of the model boundary). In the models, the density peaks and temperature minima along the flanks are the results of the magnetosheath ion entry and the subsequent $\mathbf{E} \times \mathbf{B}$ earthward convection (the FWMC model has a magnetosheath ion source only on the dawn flank, and hence the model result only shows density peak and temperature minimum along the dawn flank).

[18] As a result of the magnetosheath ion entry, plasma sheet ion distributions often have two components because

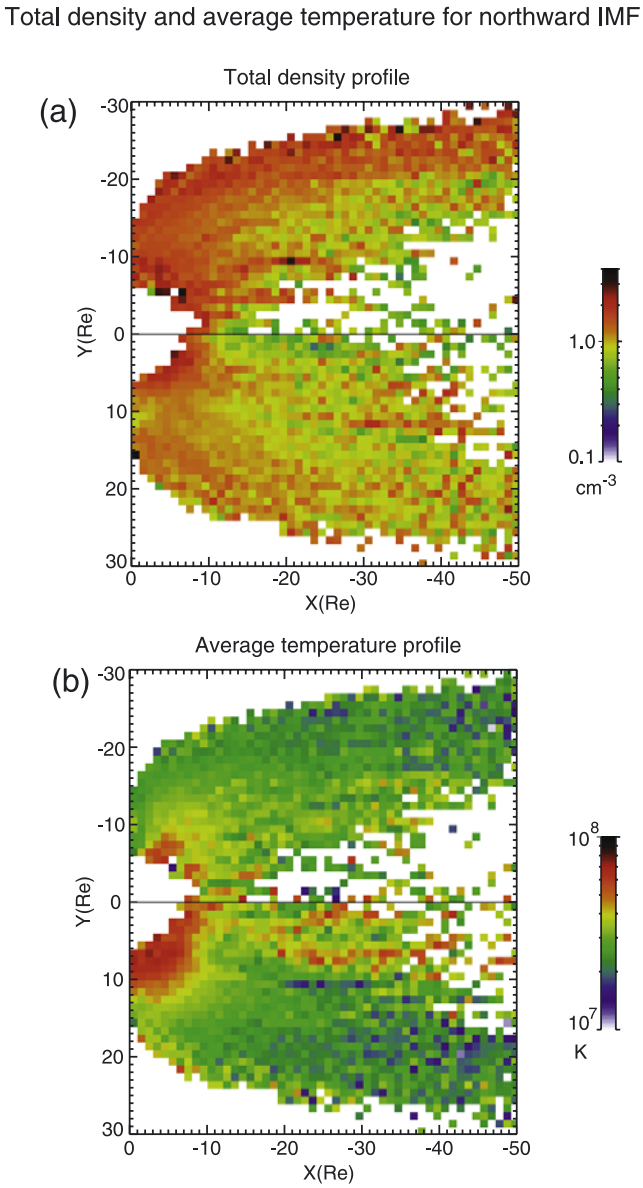

Figure 4. Two-dimensional equatorial profiles of plasma sheet ion (a) density and (b) temperature for northward IMF orientation. Each point is averaged over $1 \times 1\ R_E^2$ regions. Some regions are left blank either because of insufficient or bad data points or because plasma is anisotropic (in the region closer to the Earth).

of the mixing of the colder magnetosheath ions and hotter nominal plasma sheet ions, but in some regions, particularly along the dawn flank, many often appear to have only one component [*Fujimoto et al.*, 1998; *Hasegawa et al.*, 2003, 2004a]. As mentioned in section 3, our method fits the ion spectra with three distribution functions: (1) one-component Maxwellian, (2) two-component Maxwellian, and (3) κ distributions, and the best fit is selected. Thus the method is intrinsically good for studying the characteristics of these three types of distribution in the plasma sheet. Figure 5 shows the probability of observing each ion distribution type in the northward IMF plasma sheet profile shown in Figure 4. Figure 5 shows that by and large, the two-component distribution dominates. There is a dawn-dusk asymmetry in the two-component ion population. The two-component distribution is more frequently found along the dusk flank (probability ~70–80%), than along the dawn flank (probability ~40–50%). In contrast, the κ distribution

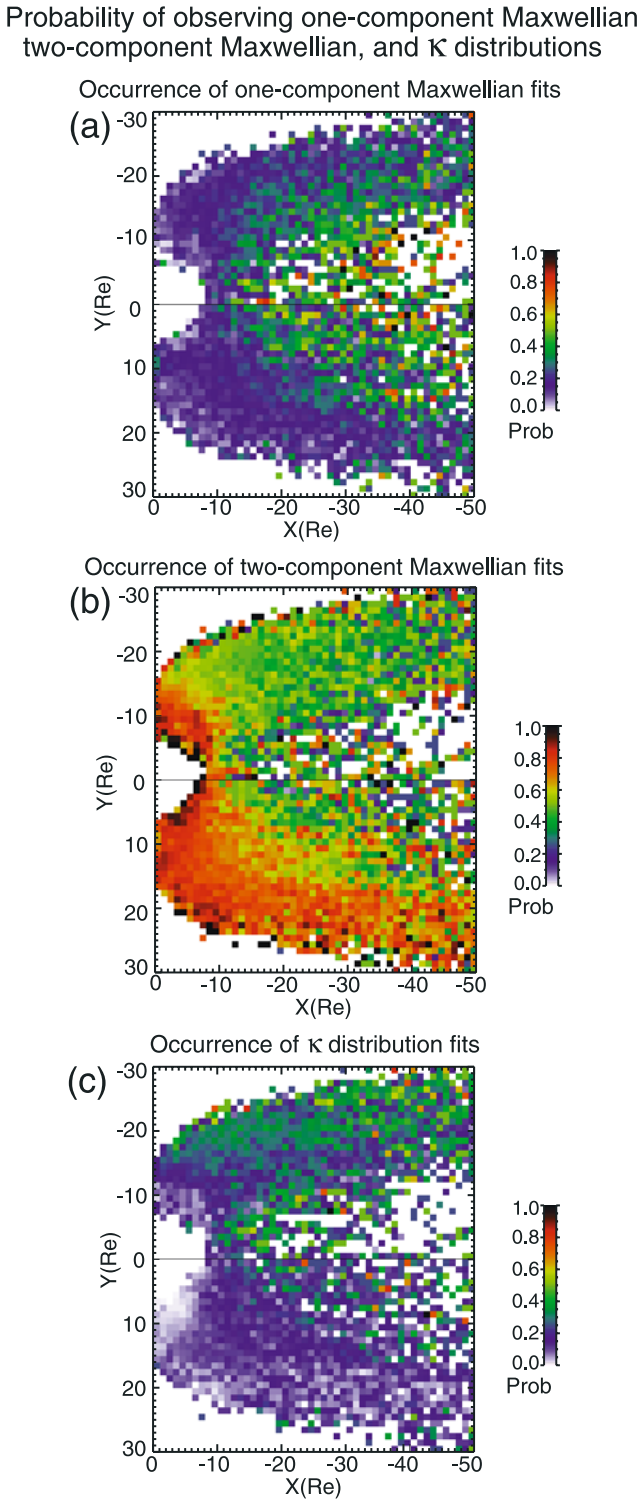

Figure 5. Probability of observing (a) one-component Maxwellian, (b) two-component Maxwellian, and (c) κ distributions in the northward IMF plasma sheet ion profiles shown in Figure 4.

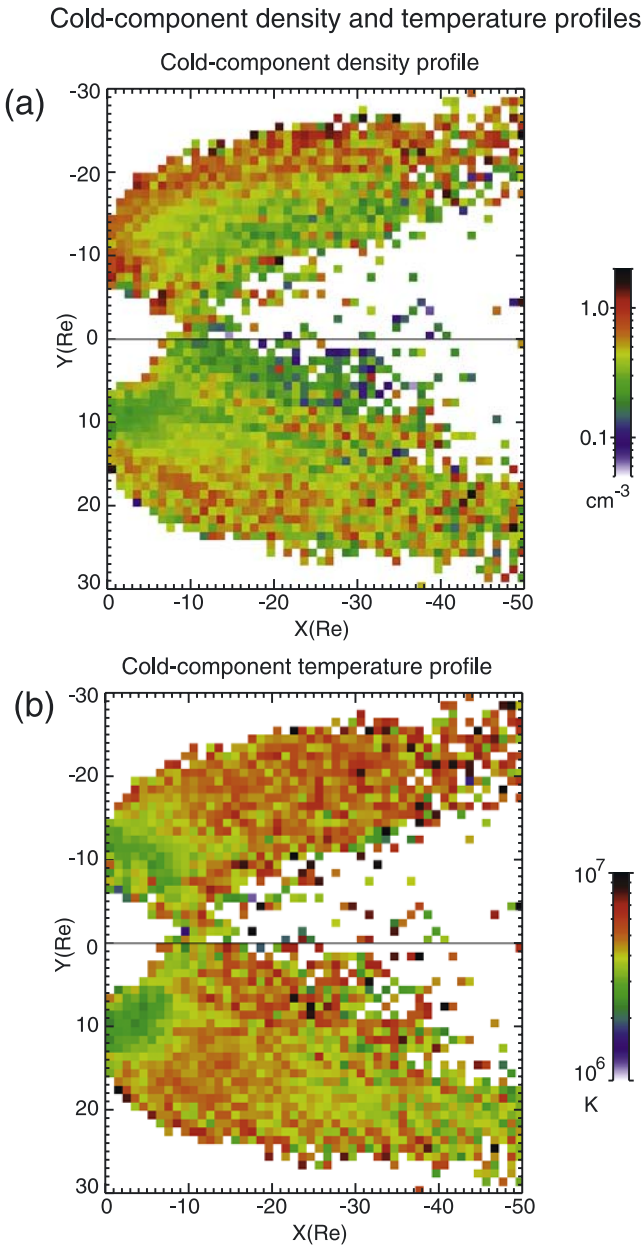

Figure 6. (a) Density and (b) temperature profiles of the cold component of the two-component Maxwellian distribution of the plasma sheet ions. Note the dawn-dusk asymmetry in the temperature profile, with the dawn flank ions having higher temperatures than the dusk flank ions. Note that the temperature scale is an order of magnitude lower than that used in other temperature profiles shown in the present paper.

has the opposite dawn-dusk asymmetry, with the dawn flank having higher probability (~30–40%) than the dusk flank (~<10%). The one-component Maxwellian distribution has a slightly higher probability along the dawn flank (~10–20%) than the dusk flank (~<10%), but it has the highest probability in the region closer to the center (midnight meridian) of the plasma sheet (~30–50%). The overall picture presented in Figure 5 is consistent with the Geotail observations in Figure 2 in that (1) there is a higher probability of observing two-component distribution along the dusk flank than along the dawn flank and (2) conversely, there is a higher probability of observing one-component distribution along the dawn flank than along the dusk flank.

[19] Because the two-component Maxwellian fit separates the distribution into hot and cold components, the properties of these two components can be investigated individually. Figure 6 presents the density and temperature of the cold component of the two-component Maxwellian distribution, which dominates the plasma sheet, particularly in the dusk sector as shown in Figure 5. Figure 6a shows that the density has maxima along both flanks, which suggests that the source and the entry points of this cold component lie along and near the magnetopause (see model calculations of *Wang et al.* [2001, 2002, 2003] and *Spence and Kivelson* [1993]). Figure 6b shows that the cold component temperature is similar to that of the magnetosheath [*Fujimoto et al.*, 1998]. However, there is a dawn-dusk asymmetry. The temperature at the dawn flank is higher than at the dusk flank. This difference is consistent with the Geotail observations that suggest that the dawnside magnetosheath ions have been heated (for example, in Figures 1 and 2). The dawn-dusk temperature asymmetry can be seen clearly in the 1-D slice along the Y direction for $X = -29$ to -31 R_E plotted in Figure 7. Figure 7 shows that the average dawn flank temperature is just slightly above 5×10^6 K, whereas the average dusk temperature is just slightly below 4×10^6 K. Thus the dawn flank magnetosheath ion appears to have been heated by about 1×10^6 K or by roughly 30–40%. It should be noted that these temperatures are consistent with the magnetosheath component of the observed distribution functions shown in Figure 1 (characteristic $v_\perp \sim 3 \times 10^2$ km/s and $T \sim 5.4 \times 10^6$ K).

[20] Figure 8 presents the density and temperature for the hot component of the two-component Maxwellian distribution. Figure 8a shows that, unlike in the density profile of the cold component (Figure 6a), there is no density peak along the flanks or density gradient in the Y direction in the

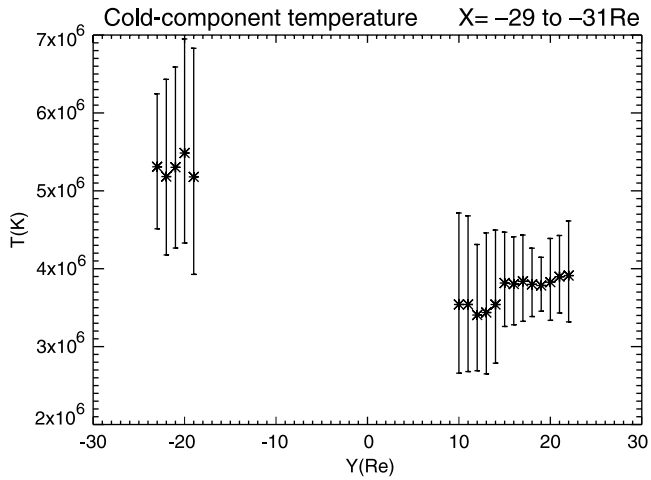

Figure 7. Cold component of the two-component Maxwellian distribution profile in the Y direction for $X = -29$ to -31 R_E. The higher dawn flank temperature is consistent with the Geotail observations that suggest the magnetosheath ions have been heated along the dawn flank during the entry process, as shown in Figures 1 and 2.

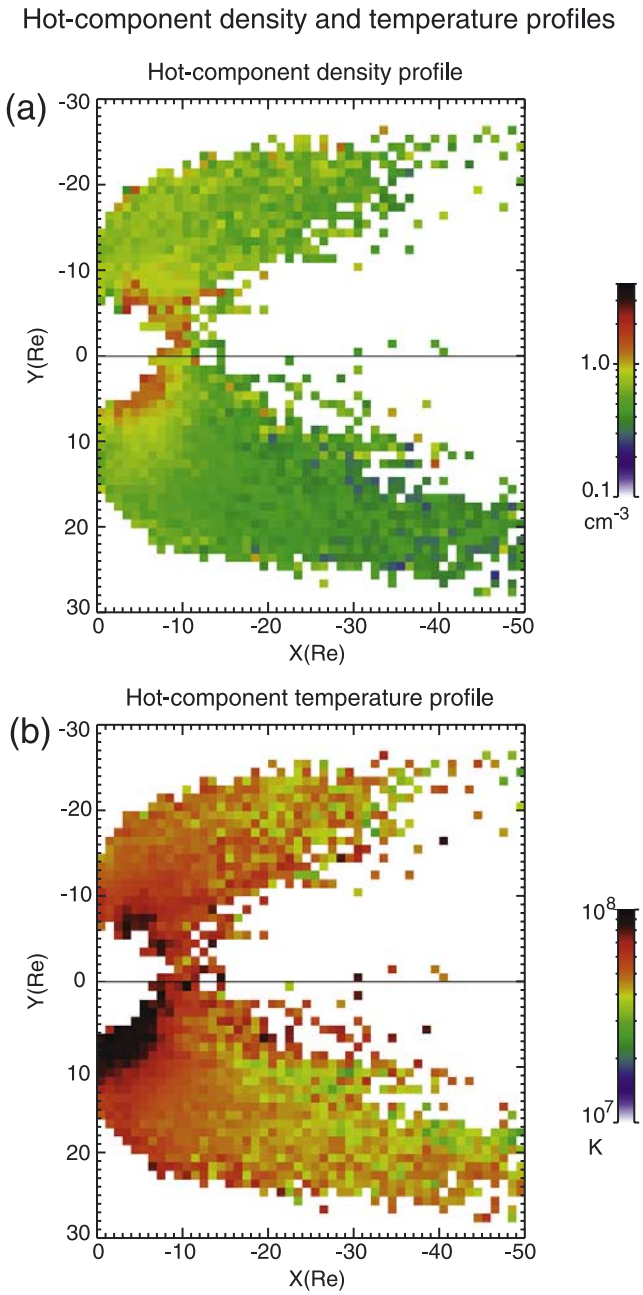

Figure 8. (a) Density and (b) temperature profiles of the hot component of the two-component Maxwellian distribution of the plasma sheet ions.

profile for the hot component. This suggests that the source for the hot component is different from that for the cold component. The hot component is believed to be of magnetospheric origin, and Figure 8a provides evidence that its source is not along the magnetopause. Figure 8b shows that the temperature of the hot component is several times higher than that of the cold (magnetosheath) temperature, typical of the nominal plasma sheet temperature [e.g., *Lennartsson and Shelley*, 1986; *Baumjohann et al.*, 1989; *Huang and Frank*, 1994; *Fujimoto et al.*, 1998]. As discussed in section 6.1.2, Figure 8b does not show much temperature dawn-dusk asymmetry along the flanks, but it is entirely possible that the actual average dawn flank temperature is lower than shown in Figure 8b, a consequence of a bias toward higher temperature of the hot component in the selection process of the two-component distribution.

[21] The κ distribution density and temperature profiles are presented in Figure 9. Figure 9 also shows a dawn-dusk asymmetry. The density is higher and the temperature is lower in the dawn sector compared with those in the dusk sector. Thus the density and the temperature have opposite asymmetry.

[22] Figure 10 presents the density and temperature profiles for one-component Maxwellian distributions. The temperature and density have the same dawn-dusk asymmetry as those for the κ distribution. It is interesting to note

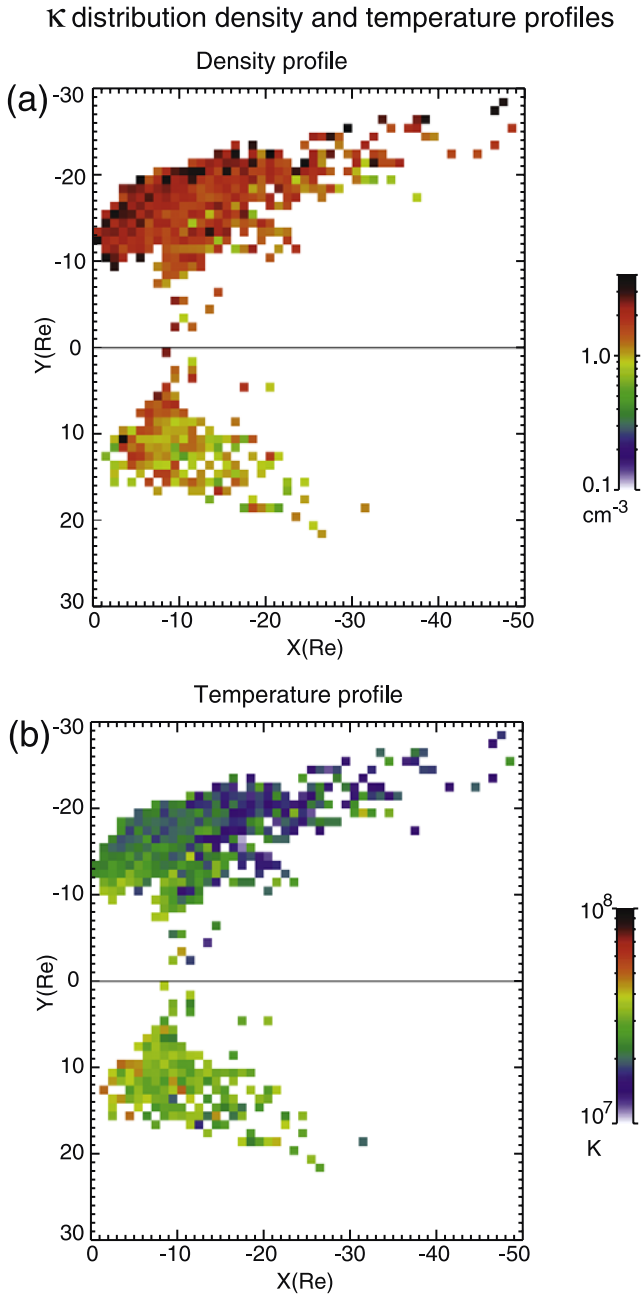

Figure 9. (a) Density and (b) temperature profiles of the κ distribution of the plasma sheet ions.

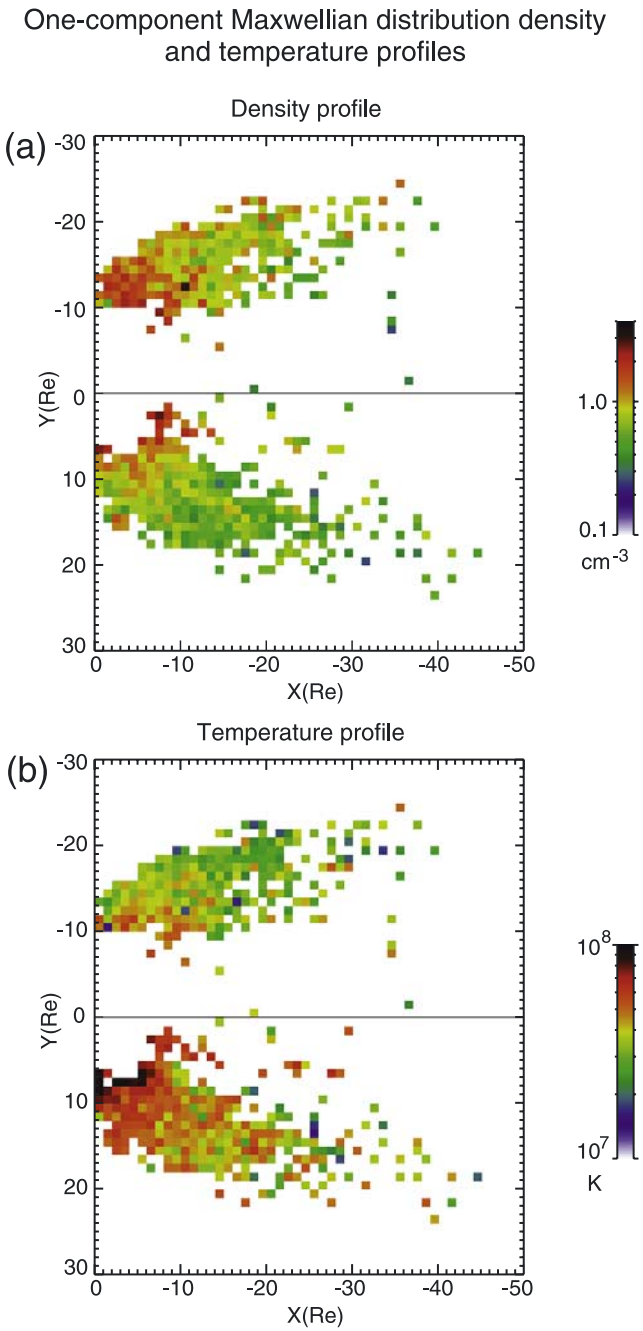

Figure 10. (a) Density and (b) temperature profiles of the one-component Maxwellian distribution of the plasma sheet ions.

that on the dawnside, the temperature lies between the typical values of the hot and cold components of the two-component distribution, but on the duskside, it is closer to the hot-component temperature.

5. Evolution of the Northward IMF Plasma Sheet Density and Temperature

[23] Section 4 presents the statistical northward IMF plasma sheet density and temperature profiles constructed from the DMSP data when the simultaneous hourly averaged IMF is northward. With our method, DMSP satellites can provide good coverage of plasma sheet density and temperature data points, albeit inferred, in a relatively short time compared to the in situ satellites. Thus the statistical global evolution of the plasma sheet density and temperature as IMF turns northward and remains northward for many hours can be reasonably investigated. The 2-D density and temperature profiles when the hourly averaged IMF has been northward for 1 to 10 hours were constructed from the 1992 DMSP data set (not shown). This sequence of figures confirms that the plasma sheet gets colder and denser the longer the IMF has been northward. In the present data set, the dawn and dusk flanks between $X = -15$ and -30 R_E have fairly good coverage and, therefore, their statistical temperature and density evolution can be studied in more detail.

[24] Figure 11 plots the dawn and dusk flank total density and temperature as the hourly averaged IMF has been northward for 1 to 10 hours (Δt = 1 to 10 hours). The density and temperature plotted are the median for the dawn and dusk flanks that are enclosed by $X = -15$ to -30 R_E; and $Y < -15$ R_E and $Y > 15$ R_E, respectively. It reconfirms that the plasma sheet gets colder and denser as IMF remains northward from 1 to 10 hours. The dawn temperature appears to reach a minimum threshold at about Δt = 5 hours, while the dusk temperature seems to continue to fall.

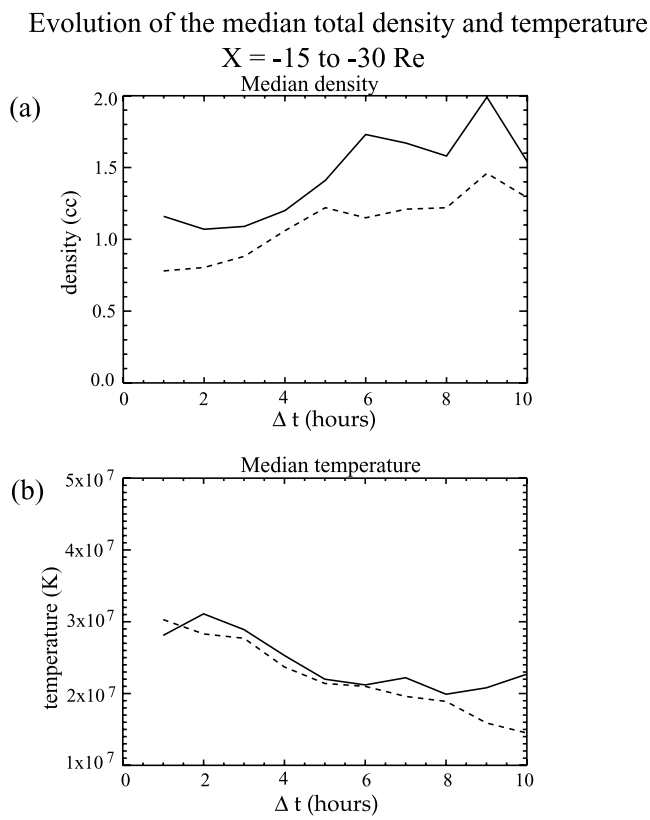

Figure 11. Evolution of the median total density and temperature in the dawn and dusk flanks as a function of Δt, where Δt is the number of hours that hourly averaged IMF has been northward. The solid line is for the dawn flank, which is defined as $Y < -15$ R_E, and the dashed line is for the dusk flank, which is defined as $Y > 15$ R_E. Both regions are bounded in X from -15 to -30 R_E.

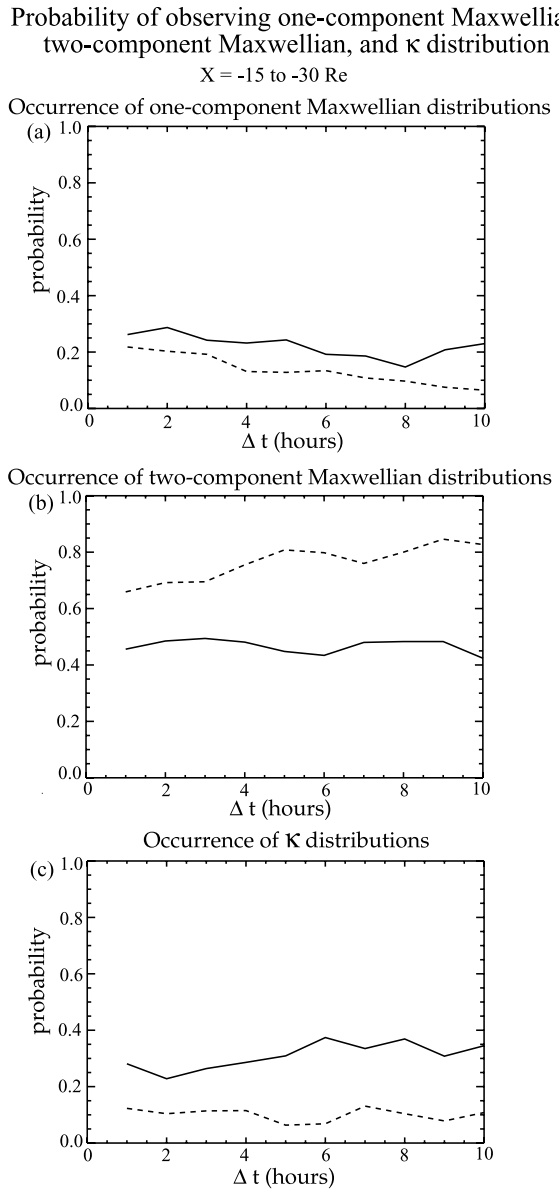

Figure 12. Average probability of observing ions having (a) one-component Maxwellian, (b) two-component Maxwellian, and (c) κ distributions in the dawn and dusk flanks as a function of Δt, where Δt is the number of hours hourly averaged IMF has been northward. The solid and dashed lines are for the dawn and dusk regions as defined in Figure 11.

There is a density dawn-dusk asymmetry with the dawn density being higher than the dusk density, but the temperature appears to be nearly symmetrical.

[25] Figure 12 plots the probability of observing the three distribution types as Δt increases from 1 to 10 hours. Figure 12b shows clearly the dawn-dusk asymmetry in the ions having two-component distribution. In the dusk flank, the probability of observing the two-component ions increases from approximately 65% to 83%, as Δt increases from 1 to 10 hours. In contrast, in the dawn flank, the probability of observing the two-component ions remains more or less constant at about 45%, which seems to be the background two-component population. The κ distribution probability, on the other hand, shows the opposite behavior. The dusk flank probability remains more or less constant at approximately 10%, while the dawn flank probability increases from approximately 25% to 35% as Δt increases from 1 to 10 hours. Thus the impact of the magnetosheath ion entries is primarily to increase the proportion of ions having κ distribution along the dawn flank and two-component distribution along the dusk flank. The occurrence of the one-component ion population steadily declines with increasing Δt, as this ion population is replaced with ions having κ and two-component distributions.

[26] It is also interesting to compare the evolution of the cold and hot components of the two-component ion population. Figure 13 plots the evolution of the median density and median temperature of the two constituents of these ions. Figures 13a and 13b show that the cold-component density on both flanks continues to increase the longer IMF has been northward, while the temperature remains more or less constant. The constant temperature is consistent with the source of the cold component being the magnetosheath, because the magnetosheath ion temperature is not expected to change with the duration of northward IMF. However, it does show the same dawn-dusk asymmetry that suggests that the dawnside magnetosheath ions have been heated by roughly $\sim 10^6$ K, as discussed in section 4. Figures 13c and 13d show that the density of the hot component remains more or less constant, whereas the temperature decreases as Δt increases from 1 to 10 hours. This evidence suggests that the plasma sheet ion cooling results not only from more magnetosheath ion entries, but also from the cooling of the nominal plasma sheet ions. Presently, it is not clear what causes the nominal plasma sheet ion temperature to decrease. Section 6.1.2 suggests some possible mechanisms. The cold and hot ion constituents are present in roughly the same quantity in the first 5 hours after northward IMF turning, but thereafter the cold ions begin to outnumber the hot ions, as seen in Figures 13a and 13c. Figures 13a and 13c suggest that the plasma sheet densification can be attributed mainly to the increase in the magnetosheath ions.

[27] In order to determine whether the variability in the solar wind plays any role in the features seen in Figures 11, 12, and 13, the average solar wind density, speed, and IMF for the selected events in Figures 11, 12, and 13 as a function of Δt are plotted in Figure 14. The plotted solar wind parameters are all very much within the range of the normal solar wind values. The average IMF *By* tends to be slightly positive, but this can be expected from averaging just one year or less of IMF data. The density for $\Delta t = 10$ shows a sudden drop, which is likely statistical resulting from having fewer available points. Apart from the density drop at $\Delta t = 10$, there is no significant/sudden jump in the average solar wind/IMF parameters as Δt increases from 1 to 10 hours. The present study ignores any feature that is based on $\Delta t = 10$.

6. Discussion and Summary

6.1. Northward IMF Plasma Sheet Ion Constituents and the Dawn-Dusk Asymmetries

[28] There are many dawn-dusk asymmetries in the plasma sheet ion profiles. The gradient and curvature drift

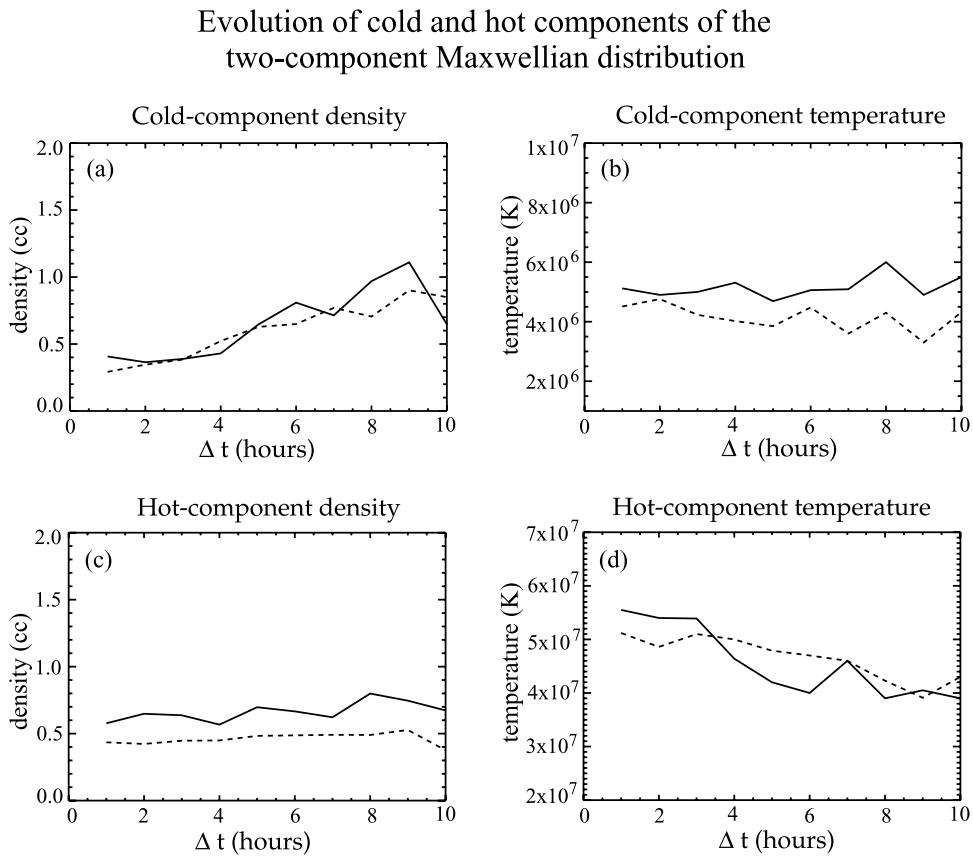

Figure 13. Evolution of the plasma sheet cold and hot components of the ions having two-component Maxwellian distribution for $X = -15$ to -30 R_E as a function of Δt, where Δt is the number of hours that hourly averaged IMF has been northward. The solid line is for the dawn flank, which is defined as $Y < -15$ R_E, and the dashed line is for the dusk flank, which is defined as $Y > 15$ R_E. Cold-component (a) median density and (b) median temperature and hot-component (c) median density and (d) median temperature.

creates higher pressure and temperature in the dusk-midnight than in the midnight-dawn sectors in the inner plasma sheet at approximately 8–10 R_E, depending on the magnetic activity level. Apart from this transport induced dawn-dusk asymmetry, less explored are the dawn-dusk asymmetries resulting from the ion sources, which is the focus of the present study.

[29] This study investigates the nature of the dawn-dusk asymmetry of the plasma sheet ions during periods of northward IMF. Previous studies with in situ observations report that frequently the plasma sheet ion population consists of two components [*Fujimoto et al.*, 1998; *Hasegawa et al.*, 2003, 2004a]. Because our method fits the ion spectra, instead of the more common moment calculation, the plasma sheet ion constituents readily come out in our analysis.

6.1.1. Cold (Magnetosheath) Component of the Two-Component Distribution

[30] When the hot and cold components are sufficiently separated in temperature, the ions fit two-component distributions. The magnetosheath origin of the cold component is evidenced in several key observations.

[31] 1. The temperature of a few ($\sim$ 4–6) 10^6 K is typical of the magnetosheath ion temperature [e.g., *Fujimoto et al.*, 1998] (Figures 7 and 13b).

[32] 2. The temperature is fairly independent of the duration of the northward IMF (Δt) (Figure 13b).

[33] 3. There are density peaks along both flanks (Figure 6), which can be taken as a signature for entries along the flank magnetopause/low-latitude boundary layer (LLBL) [*Wang et al.*, 2001, 2002, 2003; *Spence and Kivelson*, 1993].

[34] 4. The density of the cold component increases with Δt (Figure 13a).

[35] There is a dawn-dusk asymmetry in the cold component density profile, with the dawnside density being higher than the duskside density (Figure 6a). This may result from the dawn-dusk asymmetry in the magnetosheath density profile [e.g., *Paularena et al.*, 2001] and/or from entry mechanisms that favor the dawnside entries, as discussed in section 6.2.

[36] Most interestingly, there is a dawn-dusk asymmetry in the temperature profile (Figure 7). The temperature is higher in the dawn flank than in the dusk flank, which is consistent with the Geotail observations that suggest that the magnetosheath ions have been heated, perhaps during the entry process [*Hasegawa et al.*, 2003, 2004a; *Fujimoto et al.*, 1998]. The rate of density increase with Δt in the dawn flank is not uniform, as indicated in Figure 13a. In the first few ($\sim$4) hours, the rate of increase is fairly small, but

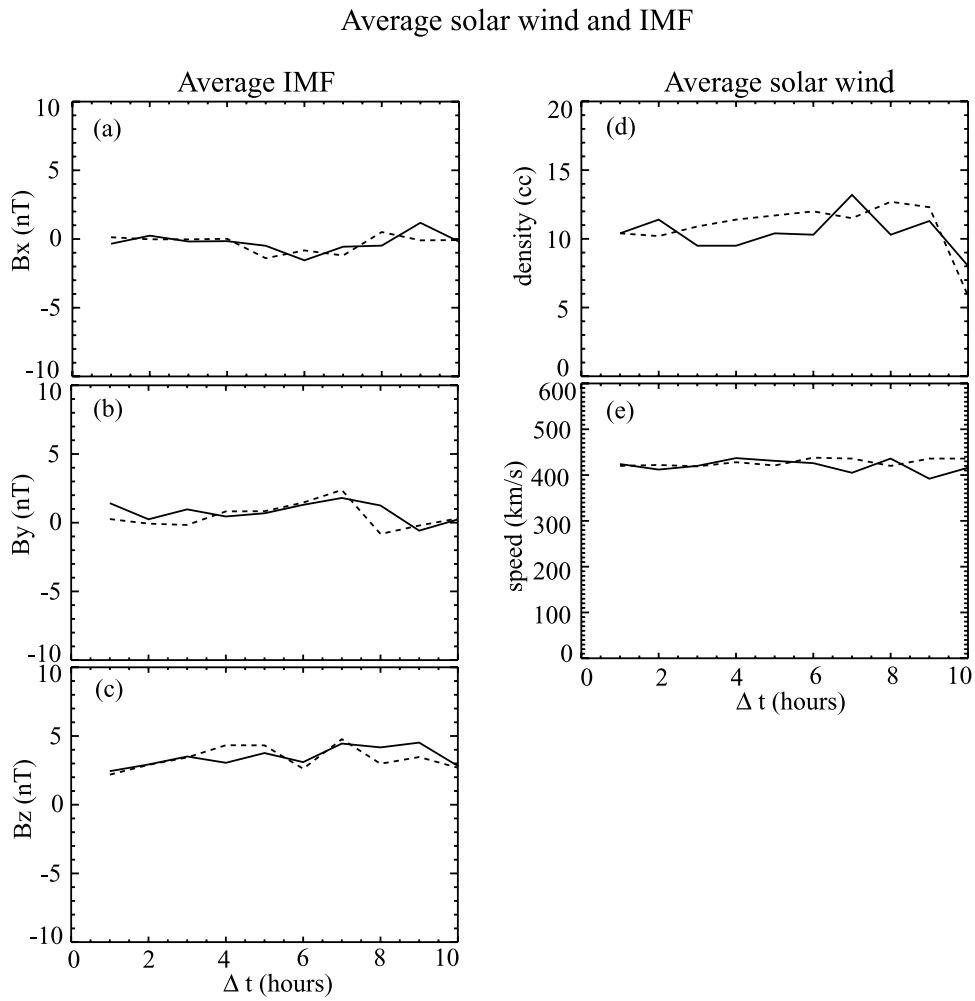

Figure 14. Average solar wind and IMF parameters during the intervals when Δt = 1 to 10 hours. (a) Average IMF Bx, (b) the average IMF By, (c) IMF Bz, (d) solar wind density, and (e) solar wind speed. The solid and dashed lines are for the data points in the dawn and dusk regions as defined in Figure 11.

thereafter it is higher (up to ~0.1 cm^{-3}/hour). This suggests that the mechanisms that brings magnetosheath ions into the magnetotail may become more effective after a few hours of northward IMF.

6.1.2. Hot (Nominal Plasma Sheet) Component of the Two-Component Distribution

[37] The hot component of the two-component distribution is most likely the nominal plasma sheet ion population. It has the following properties:

[38] 1. The temperature of a few 10^7 K is several times that of the cold component and is consistent with that of the nominal plasma sheet population [e.g., *Lennartsson and Shelley*, 1986; *Baumjohann et al.*, 1989; *Huang and Frank*, 1994; *Fujimoto et al.*, 1998].

[39] 2. The density profile in Figure 8a shows the absence of the peaks along the flanks, suggesting the source is not likely the flank magnetopause.

[40] 3. The density of the hot component is relatively insensitive to the duration of the northward IMF (Δt) and, therefore, insensitive to the influx of the magnetosheath ions (Figure 13c).

[41] Taken together, Figures 13a and 13c provide observational evidence suggesting that the densification of the plasma sheet during periods of northward IMF results entirely or almost entirely from the magnetosheath ion entries.

[42] The temperature of the hot component in the two-component distribution, as shown in Figures 8b and 13d, has little or no dawn-dusk asymmetry along the flanks. The lack of asymmetry in the average hot population temperature is somewhat puzzling on the basis of a physical argument: The magnetic field gradient and curvature drift of hot particles would tend to push higher-energy particles toward the dusk flank, which would lead to an asymmetry in the temperature of the distributions. Such an asymmetry is observed in the one-component Maxwellian and κ distributions as evidenced in Figures 9 and 10. Moreover, such dawn-dusk asymmetry is consistent with the Geotail observations in Figure 2, which shows that, on average, the hot-component (red dot) and one-component (black dot) peak temperatures are higher in the dusk flank than in the dawn flank.

[43] The lack of temperature asymmetry in the hot component of the two-component distribution may result from the selection process that introduces a bias, because identification of a distribution as having two components requires that the hot and cold components be adequately separated in

temperature/energy. Therefore the selection process would bias toward hot component with larger temperatures. Those with lower temperature would form (apparent) one-component distributions. This process operates on both the dawn and the dusk flanks. However, there are far more one-component distributions on the dawn flank than the dusk flank (Figures 5 and 12). Indeed, on the dusk flank, the occurrence of the two-component distributions is between 65% and 83%, whereas its counterpart on the dawn flank is only around 45%. Therefore, in Figures 8b and 13d, the actual average dawnside temperature should be lower, while the duskside temperature should be very close to what is shown. Also, on the dawn flank where the temperature of the cold component is higher, the hot component temperature must also be higher than normal in order to be recognized as distinct from the cold population. Hence the absence of significant temperature asymmetry in the hot component of the two-component distributions (as shown in Figures 8b and 13d) should not be considered as a contradiction to physical intuition.

[44] One interesting finding in this study is that the hot-component temperature decreases the longer the IMF has been northward (increases in Δt). The reasons for this decrease are not entirely clear. It may result from interactions between the hot and cold components mediated by waves. The interactions would cool the hot population and heat the cold population. However, the heating of the cold population, if it occurred, would not be easily observable because of the continuing, large influx of the cold magnetosheath ions as Δt increases. Figure 13 shows that the densities of the hot and cold components are initially comparable, but, as Δt increases from 1 to 10 hours, the cold-component density doubles while the hot-component density remains relatively unchanged. It is also possible that most of the hot-component energy is converted to waves, leaving the temperature of the cold population relatively unchanged. These hypotheses could be investigated using observations of wave activity in the plasma sheet. Another possibility that does not involve energy exchange between the cold and hot population is that the hotter ions in the hot population are lost through ionospheric precipitation. The hotter ions have higher speeds and bounce frequencies and hence higher loss rates. Incidentally, since electrons have higher speeds than ions, this mechanism can perhaps explain the observed lower electron than ion temperatures in the plasma sheet. The cooling of the hot component can also result from the larger magnetospheric volumes. Curvature and gradient drift offers yet another possible mechanism for the loss of the hotter ions in the hot ion population. However, Figure 13c suggests that the density of the hot component is relatively insensitive to Δt. Therefore, in the long run, the loss of the hotter ions has to be balanced by new influx of nominal plasma sheet ions, probably originating from the region further down the tail.

[45] Thus the result suggests that the cooling of plasma sheet ions with increasing Δt can be attributed to two factors: (1) the entry of cold magnetosheath ions into the plasma sheet, which is a big effect, and (2) the cooling of the nominal hot plasma sheet ions themselves.

6.1.3. The κ Distribution

[46] The κ distribution is the most likely candidate to describe the ions when the distribution has a high-energy tail. When there is a significant cold ion population, the nominal plasma sheet ions are fitted either as a separate Maxwellian (in two-component distribution) or as the high-energy tail of the cold ion distribution (in κ distribution). The selection process would favor the κ distribution when the cold ions are heated and/or the nominal plasma sheet ions are cooler. On the dawn flank, it is expected that the hot ion temperatures would normally be lower than on the dusk flank because of the gradient and curvature drifts that move hotter ions duskward. Moreover, on the dawn flank, the cold ions typically have higher temperatures (Figure 7). Therefore it is more likely that κ distributions would be observed on the dawn flank, as shown in Figures 5 and 12, where the temperatures are less distinguishable. In the dawn flank, as Δt increases, the probability of observing two-component distributions does not change much, but the probability of observing κ distributions increases (Figure 12). The majority of the hot and cold components apparently do not thermalize, since they form one-component κ rather than Maxwellian distributions.

[47] The density and temperature profiles of ions having a κ distribution show a dawn-dusk asymmetry, as indicated in Figure 9. The average temperature lies between the average temperatures of the hot and cold components when the selection process identifies two-component distributions. The temperature is lower in the dawn flank than in the dusk flank, and is apparently dominated by the hot plasma sheet ions, which would exhibit such asymmetry due to their gradient and curvature drifts. If the pressure were dominated by the cold plasma, the opposite temperature asymmetry (such as the one seen in Figures 6b and 7) would be expected.

[48] Figures 12c and 5c suggest that there are background ions with κ distributions that may form independently of the magnetosheath (cold) ions.

6.1.4. One-Component Maxwellian Distribution

[49] In the DMSP SSJ4 data, the one-component Maxwellian ions are most likely the nominal or ambient plasma sheet ions, as suggested by the following observations.

[50] 1. One-component Maxwellian distributions seem to be more abundant (have higher occurrence) in the region near the midnight meridian, away from the flanks (Figure 5).

[51] 2. The dusk flank temperature is fairly close to that of the hot component of the two-component distribution (Figures 8 and 10). In Figure 10, the temperature is lower in the dawn flank than in the dusk flank, but this asymmetry would be expected from the gradient and curvature drift that moves the hotter ions toward the dusk.

[52] 3. From the limited observations, it appears that the duration of northward IMF and the influx of magnetosheath ions have little effect on the densities of ions having one-component Maxwellian distributions. This can be seen in Figure 15, which shows that the dawn and dusk densities are relatively insensitive to Δt, at least for $\Delta t = 1$ to 6 hours. There are fewer occurrences of one-component Maxwellian distributions, especially for larger Δt. In order to improve the statistics, Figure 15 plots the densities for $X = -10$ and $-30\ R_E$, instead of $X = -15$ and $-30\ R_E$ as in Figures 11–13. Despite including data from larger regions, the statistics are still poor for large Δt, which introduces fluctuations in the dawn density at $\Delta t > 6$ hours.

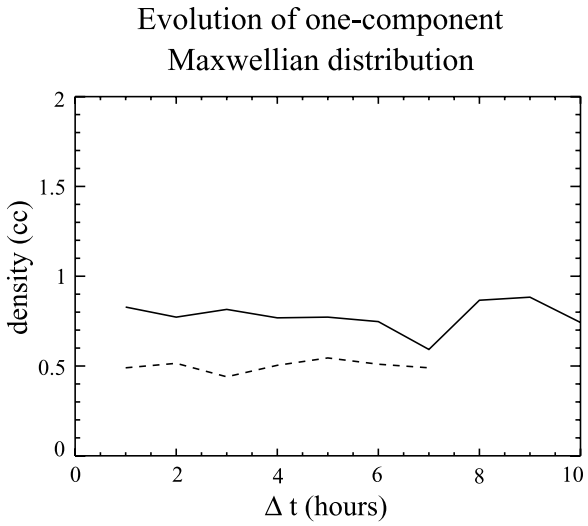

Figure 15. Evolution of the one-component Maxwellian ion median density for $X = -10$ to -30 R_E as a function of Δt, where Δt is the number of hours that hourly averaged IMF has been northward. The solid line is for the dawn flank, which is defined as $Y < -15$ R_E, and the dashed line is for the dusk flank, which is defined as $Y > 15$ R_E. The dusk density for $\Delta t > 7$ is not plotted because of lack of data points. The fluctuations in the dawn density at $\Delta t > 6$ can be attributed to poor statistics.

[53] In DMSP SSJ4 data, because of its energy range of 30 eV to 30 keV, one-component κ distributions with $\kappa > \sim 10$ would be hardly distinguishable from one-component Maxwellian distributions.

6.1.5. Comparisons of the Hot and Cold Components With in Situ Measurements

[54] Although many aspects of our results are consistent with Geotail observations shown in Figure 2, there is one key difference. Our study finds that the probability of observing ions having two components in the dawn flank is around 45% (this probability does not increase with Δt) whereas visual inspection of Figure 2 would give a lower number. This may be attributed to the two different methods of obtaining two- versus one-component distribution. Our method fits the spectra with κ, one-, and two-component Maxwellian distributions, whereas *Hasegawa et al.* [2004a] identify ions as having two components if their spectra have two energy peaks: one above and one below 3 keV. For example, the distribution with the hot-component temperature below 3 keV would not be classified as a two-component distribution in their scheme but could possibly be classified as a two-component distribution in our scheme, provided that there is enough temperature separation between the hot and cold components. Nonetheless, despite the two different methods employed in the two studies, many features in Figure 2 are consistent with our results, as mentioned throughout sections 4, 5, and 6.

6.2. Implications for Magnetosheath Ion Entry Mechanisms

[55] The dawn-dusk asymmetry and the rate of change of the two ion components can help determine the roles of the various proposed mechanisms for entry of the magnetosheath ions. Presently, there are four popular proposed mechanisms for magnetosheath ion entry: (1) high-latitude cusp reconnection at both hemispheres; (2) Kelvin-Helmholtz instability; (3) wave-induced diffusion, e.g., kinetic Alfvén waves; and (4) gradient and curvature drift. Each of these is discussed next with respect to the current findings.

[56] Ionospheric outflows, of course, contribute to the plasma sheet plasma, but during quiet time, e.g., northward IMF, their contributions are thought to be at minimal [e.g., *Yau et al.*, 1985; *Lennartsson*, 1992; *Øieroset et al.*, 1999]. Therefore ionospheric outflows are not considered in the present study.

6.2.1. High-Latitude Cusp Reconnection

[57] One possible mechanism for capturing the magnetosheath plasma on closed field lines is through high-latitude poleward of the cusp reconnections that occur in both hemispheres, forming newly closed field lines filled with magnetosheath plasma [*Song and Russell*, 1992; *Le et al.*, 1996; *Sandholt et al.*, 1999; *Fuselier et al.*, 2002]. Magnetohydrodynamic (MHD) simulations have been performed to explore this process [*Raeder et al.*, 1995, 1997]. Recently, *Øieroset et al.* [2005] report a fairly good agreement in temperature and density between an MHD simulation and Cluster satellite observations in a case study. In their MHD simulation, the plasma sheet cold ions originate from the cusp reconnection. However, it is not clear if this mechanism can introduce the observed dawn-dusk temperature asymmetry in the cold component or the observed dawn flank magnetosheath ion heating in the direction perpendicular to the magnetic field. The good agreement shown by *Øieroset et al.* [2005] and other studies suggest that reconnection plays some role in the formation of cold dense ions in the plasma sheet, but some other mechanisms may be needed to explain the observed dawn-dusk asymmetries.

6.2.2. Kelvin-Helmholtz (K-H) Instability

[58] Kelvin-Helmholtz waves grow along an inhomogeneous velocity shear layer (as found on the flank magnetopause) and eventually develop a rolled up vortex pattern in density and magnetic field. Signatures of these vortices have been found on the dusk flanks of the magnetosphere [e.g., *Fairfield et al.*, 2000; *Fujimoto et al.*, 2003]. Two-component ions have been found in the vicinity of K-H associated vortices in the dusk flank [e.g., *Fujimoto et al.*, 2003; *Hasegawa et al.*, 2004b]. Moreover, reconnection in the nonlinear stage of the K-H instability could lead to the detachment of plasma from the vortex structures, leading to significant magnetopause transport [e.g., *Otto and Fairfield*, 2000]. Hybrid simulations have indicated that ion blobs could become detached from the vortex structure of the K-H instability and could provide filaments, producing a mixing of plasma in the shear layer [*Thomas and Winske*, 1991, 1993; *Fujimoto and Terasawa*, 1994, 1995]. The electromagnetic, full-particle simulations of *Wilber and Winglee* [1995] suggest that a dawn-dusk asymmetry should be expected in the particle distributions near the magnetopause. Those simulations examined the difference between the K-H instability on the dawn and the dusk flanks. The source of the asymmetry in the simulations is the difference in the directions of the pressure gradient and the magnetic field gradient with respect to the direction of magnetosheath flow, which leads to different ∇B drift in the ions and diamagnetic drift in the plasma (non-MHD effect). The K-H

instability developed on both flanks. For the dusk flank configuration, the instability developed into vortex structures, as is observed. For the dawn flank configuration, the nonlinear wave structure was more coherent and filamentary and, in addition to plasma mixing, the ion distribution function was heated in the direction perpendicular to the magnetic field, as is commonly observed on the dawn flank (Figure 1b). This mechanism needs to be further investigated.

6.2.3. Kinetic Alfvén Waves (KAW)

[59] Large-amplitude Alfvén waves have also been observed on the magnetospheric boundary [e.g., *Tsurutani et al.*, 1982; *LaBelle and Treumann*, 1988; *Anderson and Fuselier*, 1994]. There is evidence that the waves could be the result of mode conversion of magnetosheath compressions in the sharp magnetopause gradients at the magnetopause [*Lee et al.*, 1994; *Johnson and Cheng*, 1997; *Johnson et al.*, 2001]. Because the wavelength of the mode converted waves are on the order of the ion gyroradius, they can lead to efficient convective and diffusive transport of ions across the magnetopause [*Johnson and Cheng*, 1997; *Chen*, 1999]. The waves have a parallel electric field, so they can also heat electrons in the direction of the magnetic field [*Hasegawa and Chen*, 1975; *Hasegawa and Mima*, 1978]. When the waves have large amplitudes, they can also heat ions in the direction perpendicular to the magnetic field [*Johnson and Cheng*, 2001]. Because KAW are generated when compressions interact with the magnetospheric boundary, an asymmetry could be introduced by an asymmetry in the source of the compressions. The source of compressions could be compressional instabilities generated in the magnetosheath or compressions driven directly by the solar wind. In a statistical sense, the direction of the magnetic field near the Earth is approximately Archimedes spiral, which introduces a dawn-dusk asymmetry. For this IMF orientation, *Hasegawa et al.* [2003] note that the dawnside magnetosheath magnetic field is highly fluctuating, which could indicate the presence of compressional waves. This mechanism could be investigated further by performing a survey relating compressional wave activity along the two flanks to IMF orientation.

[60] Since both KAW and K-H instability may introduce dawn-dusk temperature asymmetry in the plasma sheet cold ion constituent, further study is needed to distinguish the roles of these two mechanisms.

6.2.4. Gradient and Curvature Drift

[61] Figures 4 and 11 indicate that the density is higher along the dawn flank than along the dusk flank. In Figure 11, the dawn density is higher by about 0.2 cm^{-3} than along the dusk flank, and after a few hours of northward IMF ($\Delta t >$ ~5 hours), the density difference widens to about 0.5 cm^{-3}. Part of the higher density can be attributed to the higher density of the hot-component ions, as shown in Figure 13, but this dawn-dusk density difference is only about 0.2 cm^{-3}. Thus part of the dawn-dusk density asymmetry must also come from the cold-component ions. Indeed, this can be clearly seen in Figure 6 that shows that the cold-component ion density peak is higher along the dawn flank than along the dusk flank. The same dawn-dusk asymmetry is hinted for $\Delta t > 5$ hour in Figure 13a, which has poorer statistics (significant portions of the cold-component ions form κ distributions on the dawnside).

[62] The dawn-dusk asymmetry in the density profiles can result simply from the dawn-dusk asymmetry in the magnetosheath density profile. *Paularena et al.* [2001] report that the normalized magnetosheath density is significantly higher on the dawnside than on the duskside near solar maximum for $X = -15$ to -30 R_E. Their result would be consistent with the plasma sheet ion density dawn-dusk asymmetry obtained in this study, which used DMSP data taken near solar maximum (1992). However, *Nemecek et al.* [2003] point out that the magnetosheath dawn-dusk asymmetry is not straightforward. They report that low-latitude magnetosheath ion fluxes (FCCm [measured flux compression coefficient] = ion mass density times the bulk flow speed downstream of the bow shock divided by the same parameters upstream of the bow shock) evolve as a function of X such that on the dayside the ion fluxes are higher on the dawnside than on the duskside (similar sense as in the work by *Paularena et al.* [2001]), but the asymmetry reverses on the nightside so that ion fluxes are higher on the duskside than on the dawnside.

[63] Irrespective of the magnetosheath density dawn-dusk asymmetry, the higher density of the cold-component ions on the dawnside as compared with the duskside can be introduced by asymmetric magnetosheath ion transports across the magnetopause. Magnetosheath ions in the dawn flank can gradient and curvature drift duskward into the magnetosphere, but this entry mechanism is less effective on the dusk flank. Thus this mechanism favors more magnetosheath ion entries along the dawn flank than along the dusk flank. However, it is not clear if gradient and curvature drift alone can produce this dawn-dusk asymmetry, or if other mechanisms can also preferentially bring magnetosheath ions along the dawn flank. Most importantly, gradient and curvature drift cannot explain the observed magnetosheath ion heating in the dawn flank.

[64] The density asymmetry of the cold-component ions can provide an additional constraint to the roles of various proposed magnetosheath entry mechanisms.

7. Conclusion

[65] The variations in the plasma sheet ion spectral characteristics during northward IMF can be attributed to the dawn-dusk asymmetry in the magnetosheath ion source and gradient/curvature drift. When the temperatures of the hot nominal plasma sheet and cold magnetosheath ions are sufficiently separated or distinct from each other, the ions are identified as having two components. The two-component ions have the highest occurrence in the dusk flank, although they are present everywhere in the plasma sheet. When the temperatures of the hot and cold population are close together, they are identified as having κ distribution. Ions having κ distribution are more abundant in the dawn flank than in the dusk flank. This dawn-dusk asymmetry results from (1) the higher temperatures of the magnetosheath ions on the dawnside, consistent with the Geotail observations that suggest the dawnside magnetosheath ions have been heated [e.g., *Fujimoto et al.*, 1998; *Hasegawa et al.*, 2003, 2004a], and (2) the nominal plasma sheet ions have lower temperatures in the dawn flank than in the dusk flank, resulting from the curvature/gradient drifts that move hotter ions duskward. The observational evidence suggests

that the one-component Maxwellian ions, which can be observed most frequently near the midnight meridian, are most likely the nominal plasma sheet ions.

[66] The observations show that as IMF remains northward for longer duration (Δt increases), the plasma sheet density increases, resulting mainly from the density increase in the cold (magnetosheath) ion population. However, the cooling of the plasma sheet can be attributed to the influx of the magnetosheath ion population and the cooling of the nominal plasma sheet (hot-component) ions. The reason for the latter is not clear, but perhaps it may result from wave-mediated interactions between hot and cold populations. It is also possible that the hotter ions within the hot component deplete through some loss mechanisms with increasing Δt.

[67] The results of our study, i.e., the dawn-dusk asymmetries and the temperature and density changes with Δt, should provide constraints that can help determine the roles of various proposed magnetosheath ion entry mechanisms.

[68] **Acknowledgments.** The DMSP SSJ4 instrument was designed and built by Dave Hardy and colleagues at the AFRL. Fred Rich has been helpful in acquiring this data, as has the World Data Center in Boulder, Colorado. We thank NASA NSSDC for supplying solar wind data. We thank Masaki Fujimoto for valuable discussions. S. Wing was supported by NSF grant ATM-0344690 and NASA grants NAG5-10971 and NNG04GN14G. J. R. Johnson was supported by NSF grant ATM-0218847 and NASA grants W-19889 and NNH04AB23I.

[69] Arthur Richmond thanks Hiroshi Hasegawa and Chih-Ping Wang for their assistance in evaluating this manuscript.

References

Anderson, B. J., and S. A. Fuselier (1994), Response of thermal ions to electromagnetic ion cyclotron waves, *J. Geophys. Res.*, *99*, 19,413–19,425.

Angelopoulos, V. (1996), The role of impulsive particle acceleration in magnetotail circulation, in *Proceedings of the Third International Conference on Substorms (ICS-3), Versailles, France, 12–17 May 1996*, *Eur. Space Agency Spec. Publ.*, *ESA SP-389*, 17–22.

Angelopoulos, V., et al. (1993), Characteristics of ion flow in the quiet state of the inner plasma sheet, *Geophys. Res. Lett.*, *20*, 1711–1714.

Baumjohann, W., and R. A. Treumann (1997), *Basic Space Plasma Physics*, p. 120, Imperial Coll. Press, London.

Baumjohann, W., G. Paschmann, and C. A. Cattell (1989), Average plasma properties in the central plasma sheet, *J. Geophys. Res.*, *94*, 6597–6606.

Baumjohann, W., G. Paschmann, and H. Luhr (1990), Pressure balance between lobe and plasma sheet, *Geophys. Res. Lett.*, *17*, 45–48.

Bernstein, W., B. Hultqvist, and H. Borg (1974), Some implications of low altitude observations of isotropic precipitation of ring current protons beyond the plasmapause, *Planet. Space Sci.*, *22*, 767–776.

Bevington, P. R. (1969), *Data Reduction and Error Analysis for the Physical Sciences*, pp. 187–239, McGraw-Hill, New York.

Borovsky, J. E., M. F. Thomnsen, and R. C. Elphic (1998), The driving of plasma sheet by the solar wind, *J. Geophys. Res.*, *103*, 17,617–17,639.

Chen, L. (1999), Theory of plasma transport induced by low-frequency hydromagnetic waves, *J. Geophys. Res.*, *104*, 2421–2428.

Christon, S. P., D. G. Mitchell, D. J. Williams, L. A. Frank, C. Y. Huang, and T. E. Eastman (1988), Energy spectra of plasma sheet ions and electrons from ~50 eV/e to ~1 MeV during plasma temperature transitions, *J. Geophys. Res.*, *93*, 2562–2572.

Christon, S. P., D. J. Williams, D. G. Mitchell, L. A. Frank, and C. Y. Huang (1989), Spectral characteristics of plasma sheet ion and electron populations during undisturbed geomagnetic conditions, *J. Geophys. Res.*, *94*, 13,409–13,424.

Fairfield, D. H., A. Otto, T. Mukai, S. Kokubun, R. P. Lepping, J. T. Steinberg, A. J. Lazarus, and T. Yamamoto (2000), Geotail observations of the Kelvin-Helmholtz instability at the equatorial magnetotail boundary for parallel northward fields, *J. Geophys. Res.*, *105*, 21,159–21,173.

Fujimoto, M., and T. Terasawa (1994), Anomalous ion mixing within an MHD scale Kelvin-Helmholtz vortex, *J. Geophys. Res.*, *99*, 8601–8614.

Fujimoto, M., and T. Terasawa (1995), Anomalous ion mixing within an MHD scale Kelvin-Helmholtz vortex: 2. Effects of inhomogeneity, *J. Geophys. Res.*, *100*, 12,025–12,034.

Fujimoto, M., T. Terasawa, T. Mukai, Y. Saito, T. Yamamoto, and S. Kokubun (1998), Plasma entry from the flanks of the near-Earth magnetotail: Geotail observations, *J. Geophys. Res.*, *103*, 4391–4408.

Fujimoto, M., T. Tonooka, and T. Mukai (2003), Vortex-like fluctuations in the magnetotail flanks and their possible roles in plasma transport, in *Earth's Low-Latitude Boundary Layer*, *Geophys. Monogr. Ser.*, vol. 133, edited by P. Newell and T. Onsager, pp. 241–251, AGU, Washington, D. C.

Fuselier, S. A., J. Berchem, K. J. Trattner, and R. Friedel (2002), Tracing ions in the cusp and low-latitude boundary layer using multispacecraft observations and a global MHD simulation, *J. Geophys. Res.*, *107*(A9), 1226, doi:10.1029/2001JA000130.

Hardy, D. A., L. K. Schmitt, M. S. Gussenhoven, F. J. Marshall, H. C. Yeh, T. L. Shumaker, A. Hube, and J. Pantazis (1984), Precipitating electron and ion detectors (SSJ/4) for the block 5D/flights 6-10 DMSP satellites: Calibration and data presentation, *Rep. AFGL-TR-84-0317*, Air Force Geophys. Lab., Hanscom Air Force Base, Mass.

Hasegawa, A., and L. Chen (1975), Kinetic process of the plasma heating by Alfven wave, *Phys. Rev. Lett.*, *35*, 370–373.

Hasegawa, A., and K. Mima (1978), Anomalous transport produced by kinetic Alfven wave turbulence, *J. Geophys. Res.*, *83*, 1117–1123.

Hasegawa, H., M. Fujimoto, K. Maezawa, Y. Saito, and T. Mukai (2003), Geotail observations of the dayside outer boundary region: Interplanetary magnetic field control and dawn-dusk asymmetry, *J. Geophys. Res.*, *108*(A4), 1163, doi:10.1029/2002JA009667.

Hasegawa, H., M. Fujimoto, Y. Saito, and T. Mukai (2004a), Dense and stagnant ions in the low-latitude boundary region under northward interplanetary magnetic field, *Geophys. Res. Lett.*, *31*, L06802, doi:10.1029/2003GL019120.

Hasegawa, H., M. Fujimoto, T.-D. Phan, H. Rème, A. Balogh, M. W. Dunlop, C. Hashimoto, and R. TanDokoro (2004b), Transport of solar wind into Earth's magnetosphere through rolled-up Kelvin-Helmholtz vortices, *Nature*, *430*, 755–758.

Huang, C. Y., and L. A. Frank (1994), A statistical survey of the central plasma sheet, *J. Geophys. Res.*, *99*, 83–95.

Johnson, J. R., and C. Z. Cheng (1997), Kinetic Alfven waves and plasma transport at the magnetopause, *Geophys. Res. Lett.*, *24*, 1423–1426.

Johnson, J. R., and C. Z. Cheng (2001), Stochastic ion heating at the magnetopause due to kinetic Alfven waves, *Geophys. Res. Lett.*, *28*, 4421–4424.

Johnson, J. R., C. Z. Cheng, and P. Song (2001), Signatures of mode conversion and kinetic Alfven waves at the magnetopause, *Geophys. Res. Lett.*, *28*, 227–230.

Kistler, L. M., E. Mobius, W. Baumjohann, G. Paschmann, and D. C. Hamilton (1992), Pressure changes in the plasma sheet during substorm injections, *J. Geophys. Res.*, *97*, 2973–2983.

LaBelle, J., and R. A. Treumann (1988), Plasma waves at the dayside magnetopause, *Space Sci. Rev.*, *47*, 175–202.

Le, G., C. T. Russell, J. T. Gosling, and M. F. Thomsen (1996), ISEE observations of low-latitude boundary layer for northward interplanetary magnetic field: Implications for cusp reconnection, *J. Geophys. Res.*, *101*, 27,239–27,250.

Lee, L. C., J. R. Johnson, and Z. W. Ma (1994), Kinetic Alfvén waves as a source of plasma transport at the dayside magnetopause, *J. Geophys. Res.*, *99*, 17,405–17,411.

Lennartsson, W. (1992), A scenario for solar wind penetration of Earth's magnetic tail based on ion composition data from the ISEE 1 spacecraft, *J. Geophys. Res.*, *97*, 19,221–19,238.

Lennartsson, W., and E. G. Shelley (1986), Survey of 0.1- to 16-keV/e plasma sheet ion composition, *J. Geophys. Res.*, *91*, 3061–3076.

Lyons, L. R., and T. W. Speiser (1982), Evidence for current sheet acceleration in the geomagnetic tail, *J. Geophys. Res.*, *87*, 2276–2286.

Meng, C.-I., A. T. Y. Lui, S. M. Krimigis, S. Ismail, and D. J. Williams (1981), Spatial distribution of energetic particles in the distant magnetotail, *J. Geophys. Res.*, *86*, 5682–5700.

Nemecek, Z., M. Hayosh, J. Safrankova, G. Zastenker, and J. Richardson (2003), The dawn-dusk asymmetry of the magnetosheath: INTERBALL-1 observations, *Adv. Space Res.*, *31*(5), 1333–1340.

Newell, P. T., Y. I. Feldstein, Y. I. Galperin, and C.-I. Meng (1996), Morphology of nightside precipitation, *J. Geophys. Res.*, *101*, 10,737–10,748.

Newell, P. T., V. A. Sergeev, G. R. Bikkuzina, and S. Wing (1998), Characterizing the state of the magnetosphere: Testing the ion precipitation maxima latitude (b2i) and the ion isotropy boundary, *J. Geophys. Res.*, *103*, 4739–4745.

Øieroset, M., et al. (1999), Energetic ion outflow from the dayside ionosphere: Categorization, classification, and statistical study, *J. Geophys. Res.*, *104*, 24,915–24,928.

Øieroset, M., J. Raeder, T. D. Phan, S. Wing, J. P. McFadden, W. Li, M. Fujimoto, H. Rème, and A. Balogh (2005), Global cooling and densification of the plasma sheet during an extended period of purely northward IMF on October 22–24, 2003, *Geophys. Res. Lett.*, *32*, L12S07, doi:10.1029/2004GL021523.

Otto, A., and D. H. Fairfield (2000), Kelvin-Helmholtz instability at the magnetotail boundary: MHD simulation and comparison with Geotail observations, *J. Geophys. Res.*, *105*, 21,175–21,190.

Papitashvili, V. O., N. E. Papitashvili, and J. H. King (2000), Solar cycle effects in planetary geomagnetic activity: Analysis of 36-year long OMNI dataset, *Geophys. Res. Lett.*, *27*, 2797–2800.

Paularena, K. I., J. D. Richardson, M. A. Kolpak, C. R. Jackson, and G. L. Siscoe (2001), A dawn-dusk density asymmetry in Earth's magnetosheath, *J. Geophys. Res.*, *106*, 25,377–25,394.

Phan, T. D., et al. (1997), Low-latitude dusk flank magnetosheath, magnetopause, and boundary layer for low magnetic shear: Wind observations, *J. Geophys. Res.*, *102*, 19,883–19,895.

Pulkkinen, T. I., and N. A. Tsyganenko (1996), Testing the accuracy of magnetospheric model field line mapping, *J. Geophys. Res.*, *101*, 27,431–27,442.

Raeder, J., R. J. Walker, and M. Ashour-Abdalla (1995), The structure of the distant geomagnetic tail during long periods of northward IMF, *Geophys. Res. Lett.*, *22*, 349–352.

Raeder, J., et al. (1997), Boundary layer formation in the magnetotail: Geotail observations and comparisons with a global MHD simulation, *Geophys. Res. Lett.*, *24*, 951–954.

Sandholt, P. E., C. J. Farrugia, S. W. H. Cowley, W. F. Denig, M. Lester, J. Moen, and B. Lybekk (1999), Capture of magnetosheath plasma by the magnetosphere during northward IMF, *Geophys. Res. Lett.*, *26*, 2833–2836.

Sarris, E. T., S. M. Krimigis, A. T. Y. Lui, K. L. Ackerson, L. A. Frank, and D. J. Williams (1981), Relationship between energetic particles and plasmas in the distant plasma sheet, *Geophys. Res. Lett.*, *8*, 349–352.

Sergeev, V. A., and B. B. Gvozdevsky (1995), MT-index—A possible new index to characterize the magnetic configuration of magnetotail, *Ann. Geophys.*, *13*, 1093–1103.

Sergeev, V. A., M. Malkov, and K. Mursula (1993), Testing the isotropic boundary algorithm method to evaluate the magnetic field configuration in the tail, *J. Geophys. Res.*, *98*, 7609–7620.

Song, P., and C. T. Russell (1992), Model of the formation of the low-latitude boundary layer for strongly northward interplanetary magnetic field, *J. Geophys. Res.*, *97*, 1411–1420.

Spence, H. E., and M. G. Kivelson (1993), Contributions of the low-latitude boundary layer to the finite width magnetotail convection model, *J. Geophys. Res.*, *98*, 15,487–15,496.

Spence, H. E., M. G. Kivelson, R. J. Walker, and D. J. McComas (1989), Magnetospheric plasma pressures in the midnight meridian: Observations from 2.5 to 35 RE, *J. Geophys. Res.*, *94*, 5264–5272.

Stenuit, H., et al. (2002), Multi-spacecraft study on the dynamics of the dusk-flank magnetosphere under northward IMF: January 10–11, 1997, *J. Geophys. Res.*, *107*(A10), 1333, doi:10.1029/2002JA009246.

Terasawa, T., et al. (1997), Solar wind control of density and temperature in the near-Earth plasma sheet: Wind/Geotail collaboration, *Geophys. Res. Lett.*, *24*, 935–938.

Thomas, V. A., and D. Winske (1991), Kinetic simulation of the Kelvin-Helmholtz instability at the Venus ionopause, *Geophys. Res. Lett.*, *18*, 1943–1946.

Thomas, V. A., and D. Winske (1993), Kinetic simulations of the Kelvin-Helmholtz instability at the magnetopause, *J. Geophys. Res.*, *98*, 11,425–11,438.

Tsurutani, B. T., E. J. Smith, R. R. Anderson, K. W. Ogilvie, J. D. Scudder, D. N. Baker, and S. J. Bame (1982), Lion roars and nonoscillatory drift mirror waves in the magnetosheath, *J. Geophys. Res.*, *87*, 6060–6072.

Tsyganenko, N. A. (1989), A magnetospheric magnetic field model with a warped tail current sheet, *Planet. Space Sci.*, *37*, 5–20.

Vasyliunas, V. M. (1971), Deep space plasma measurements, in *Methods of Experimental Physics: Plasma Physics*, *Part B*, vol. 9, edited by R. H. Lovberg and H. R. Griem, pp. 49–88, Elsevier, New York.

Wang, C.-P., L. R. Lyons, M. W. Chen, and R. A. Wolf (2001), Modeling the quiet time inner plasma sheet protons, *J. Geophys. Res.*, *106*, 6161–6178.

Wang, C.-P., L. R. Lyons, M. W. Chen, and R. A. Wolf (2002), Two-dimensional quiet time equilibrium for the inner plasma sheet protons and magnetic field, *Geophys. Res. Lett.*, *29*(24), 2186, doi:10.1029/2001GL013984.

Wang, C.-P., L. R. Lyons, M. W. Chen, R. A. Wolf, and F. R. Toffoletto (2003), Modeling the inner plasma sheet protons and magnetic field under enhanced convection, *J. Geophys. Res.*, *108*(A2), 1074, doi:10.1029/2002JA009620.

Wilber, M., and R. M. Winglee (1995), Dawn-dusk asymmetries in the low-latitude boundary layer arising from the Kelvin-Helmholtz instability: A particle simulation, *J. Geophys. Res.*, *100*, 1883–1898.

Wing, S., and P. T. Newell (1998), Central plasma sheet ion properties as inferred from ionospheric observations, *J. Geophys. Res.*, *103*, 6785–6800.

Wing, S., and P. T. Newell (2000), Quiet time plasma sheet ion pressure contribution to Birkeland currents, *J. Geophys. Res.*, *105*, 7793–7802.

Wing, S., and P. T. Newell (2002), 2D plasma sheet ion density and temperature profiles for northward and southward IMF, *Geophys. Res. Lett.*, *29*(9), 1307, doi:10.1029/2001GL013950.

Wing, S., and P. Newell (2003), LLBL contribution to the plasma sheet ions, in *Earth's Low-Latitude Boundary Layer*, *Geophys. Monogr. Ser.*, vol. 133, edited by P. T. Newell and T. Onsager, pp. 273–282, AGU, Washington, D. C.

Yau, A., E. G. Shelley, W. K. Peterson, and L. Lenchyshyn (1985), Energetic auroral and polar ion outflow at DE-1 altitudes: Magnitude, composition, magnetic activity dependence and long-term variations, *J. Geophys. Res.*, *90*, 8417–8432.

J. R. Johnson, Princeton Plasma Physics Laboratory, Princeton University, Princeton, NJ 08543, USA.

C.-I. Meng, P. T. Newell, and S. Wing, Applied Physics Laboratory, Johns Hopkins University, Laurel, MD 20723-6099, USA. (simon.wing@jhuapl.edu)